

# A POSTERIORI CERTIFICATION FOR PHYSICS-INFORMED NEURAL NETWORKS

LEWIN ERNST, NIKOLAOS REKATSINAS, AND KARSTEN URBAN

**ABSTRACT.** We propose rigorous lower and upper bounds for a PINN approximation to PDEs by efficiently computing the Riesz representations of suitable extension and restrictions of the PINN residual towards geometrically simpler domains, which are either embedded or enveloping the original domain. Error bounds are proven and detailed for elliptic as well as parabolic problems. Numerical experiments show the good quantitative behaviour of the derived upper and lower error bounds.

## 1. INTRODUCTION

In recent years, a broad and continuous interest on the usage of neural networks for the numerical approximation of solutions to partial differential equations (PDEs) is being witnessed and vastly depicted in the literature, e.g. [1–5], where this list is far from being complete. Physics-informed neural networks (PINNs), trained with loss functions related to the residual of a given PDE, are extensively used to solve PDEs in particular posed on complex-shaped or varying domains, as a PINN avoids complicated discretization techniques and thus keeps the implementation effort low. On the other hand, however, a theory for the assessment of the approximation quality in terms of an a posteriori error control is at least not obvious, and highly unexplored compared to the wide acceptance of PINNs.

In other words, the aim of this paper is to discuss the *certification* of PINN approximations. By this, we mean the derivation of rigorous, computable lower and upper bounds on the error between the true (unknown) PDE solution and any PINN approximation. In particular, we want to avoid any assumption on the architecture, training or training data of the PINN. We view it as a given black box for the approximation of a known PDE on a known domain  $\Omega \subset \mathbb{R}^d$ . Hence, this paper is devoted to *error estimation* for PINN approximations.

A common approach to assess the accuracy of a PINN solution is to bound the approximation error by the generalization error, which measures the  $L_2$ -norm of the residual on the entire domain, not just the training points. In [6], the generalization error has been bounded in terms of the training error, the number of training samples and the quadrature error, up to constants stemming from stability estimates on the underlying PDE. Although this approach provides an instructive insight for the training process as well as the quality of the approximation, it is generally not sharp and relies on a stability assumption on the underlying PDE.

---

2020 *Mathematics Subject Classification.* 35J20, 65M15, 68T07.

*Key words and phrases.* Physics Informed Neural Networks; A Posteriori Error Bound; Parameterized Partial Differential Equations; Extension and Restriction of Functionals.

Moreover, it requires the exact solution, so this approach is inherently theoretical rather than of practical use for certification.

In [7], three key theoretical questions on PINNs error analysis are posed, in particular (i) on how small PDE residuals can be made in the class of neural networks, (ii) on whether a small residual implies a small total error and (iii) small training errors imply small total errors for sufficient number of quadrature points. Based upon these questions the authors prove a priori error estimates for a nonlinear PDE, the incompressible Navier-Stokes equation. These estimates are then used in a posteriori fashion on an example with analytical solutions to compute the theoretical bounds and assess them quantitatively. Although this analysis constitutes a comprehensive theoretical analysis of PINNs for a nonlinear PDE, assumptions on smoothness of the solution and the ability to find a global training loss minimum in order to estimate training errors somewhat limit applicability.

Unlike generalization error approaches, the methods in [8–11] provide PDE formulations that in turn define loss functionals suitable for neural network training, and which enable the computation of numerical bounds on the actual error between the neural network approximation and the true solution. [12] yields certification of the error without a priori knowledge of the solution using arguments from semi-group theory. [8] introduces a reliable and efficient error estimator for variational neural networks (VPINNs). The bound for the error consists of a residual-type term, a loss function term and a term for the data oscillation. However, the PINN approximation should follow the corresponding discretization of the PDE. In [9] rigorous a posteriori error control is constructed by connecting the residual to the approximation error with computable quantities based on a well-posed formulation of the PDE. This is achieved using wavelet expansions of the dual norm of the residual as the loss function to train the neural network. In [10] a least-squares framework for neural networks based on first-order systems of PDEs is introduced. The least squares residual serves both as a loss functional and as an a posteriori error estimator, allowing the residual to provide a computable upper bound on the approximation error. In similar spirit, the proposed least-squares formulations for PDEs in [11] provide loss functionals that achieve quasi-optimal approximation rates in appropriate norms, specifically addressing inhomogeneous boundary conditions avoiding fractional Sobolev norms.

The PINN approach relies on the assumption that training a neural network by a loss function based upon the residual gives rise to a small approximation error. This requires stability and a variationally correct form of the neural network, ensuring that the loss remains proportional to the error measured in a norm induced by the problem, [13].

**1.1. Contribution.** Viewing a PINN as a given black box, we propose a framework to rigorously bound the PINN approximation error from above and from below by quantities which can efficiently be computed a posteriori – independently of the choice of the loss functional or the configuration of training. This is achieved in the following way:

- i) starting by a well-posed (variational) formulation of the PDE on some domain  $\Omega \subset \mathbb{R}^d$ , we use a well-known error-residual relation;
- ii) choose geometrically simple domains  $\circ$  and  $\square$  such that  $\circ \subset \Omega \subset \square$ ;
- iii) extend and restrict the residual of the PINN to  $\circ$  and  $\square$  in a suitable manner;

- iv) construct computable surrogates of the dual norm of the residual on  $\bigcirc$  and  $\square$  and relate them to the residual posed on  $\Omega$ .

Our main motivation for this methodology lies on the following: Since PINNs are mesh-free, their usage is particularly attractive when the geometry of  $\Omega$  is such that forming a triangulation e.g. for a finite element discretization is computationally costly. Such a situation occurs, for instance, if  $\Omega$  is complex or if  $\Omega$  is varying depending on some parameter in such a way that mapping to some reference domain is not easily possible. Examples might include geometry or topology optimization and fluid-structure interaction. Hence, we do not make use of any discretization of the underlying PDE on  $\Omega$  (as e.g. in [8]).

However, reducing the computations for the error bounds on simpler domains  $\bigcirc$  and  $\square$ , we can use highly efficient numerical schemes.

**1.2. Organization of material.** The structure of this paper is as follows. In Section 2, we briefly revise the PINNs methodology for solving PDEs. In Section 3, we recall the variational framework for weak formulations and their practical relevance to residual-based a posteriori error control. Moreover, we review the computational techniques used to evaluate dual norms. In Section 4, we introduce the theoretical framework and prove the lower and upper bounds for the error. The abstract setting is detailed for elliptic and parabolic problems. Numerical experiments are presented in Section 5 to quantitatively investigate our numerical bounds. We conclude with a brief summary and an outlook towards potential directions for future research.

## 2. PINNS FOR SOLVING PDES

We are going to briefly introduce the main concepts of PINNs without going into details, since we only aim to use PINNs as a black box.

**2.1. PDEs in classical form.** Let  $\Omega \subset \mathbb{R}^d$  be a bounded open domain and let  $m \in \mathbb{N}$  denote the order of the PDE ( $m = 2$  for Laplace's equation). We denote by

$$B^\circ : C^m(\Omega) \rightarrow C^0(\Omega)$$

the classical (point-wise) form of the differential operator under consideration. Then, given some  $f^\circ \in C(\Omega)$ , we call  $u \in C^m(\Omega)$  a *classical solution* if

$$(2.1) \quad (B^\circ u)(x) = f^\circ(x), \quad \forall x \in \Omega,$$

where we assume that proper boundary and/or initial conditions are incorporated into the definition of the operator.

Next, we are given some approximation  $u^\delta$  to  $u$ , e.g. in terms of a PINN and define the (classical) *residual* of (2.1) by

$$(2.2) \quad r_\Omega^\circ(u^\delta)(x) := f(x) - (B^\circ u^\delta)(x), \quad x \in \Omega.$$

Given  $u^\delta$ , the residual is in principle computable by inserting  $u^\delta$  into the PDE operator.

However, such classical solutions often do not exist, depending on the data  $B^\circ$ ,  $f^\circ$  and  $\Omega$ . It is well-known that well-posedness of such problems is usually linked to suitable variational formulations as described in Section 3 below.

**2.2. PINNs: Definition and training.** The core idea of PINNs is to use the residual for the definition of a loss function within the training of a neural network. Let us briefly describe this for the above classical solution concept, even though (i) there are several other approaches in the literature and (ii) our subsequent error analysis does not depend on the choice of the loss function for a PINN.

*Neural networks (NNs).* The notation of NNs in this paragraph is based upon [14–16]. A NN is a function  $\Phi_a(\cdot; \theta) : \mathbb{R}^{N_0} \rightarrow \mathbb{R}^{N_L}$ , where  $a$  is the *architecture* and  $\theta$  are the *parameters*. Both the architecture and parameters determine the input-output function  $\Phi_a(\cdot; \theta)$  of the NN. In case of a feed-forward NN, the architecture  $a = (N, \rho)$  can be described by the vector of neurons per layer  $N = (N_0, \dots, N_L) \in \mathbb{N}^{L+1}$ , where  $L \in \mathbb{N}$  denotes the number of *layers* ( $N_0$  being the input and  $N_L$  the output dimension) and the *activation function*  $\rho : \mathbb{R} \rightarrow \mathbb{R}$ .

The parameters of the NN read  $\theta = (W^{(l)}, b^{(l)})_{l=1, \dots, L}$ , where  $W^{(l)} \in \mathbb{R}^{N_l \times N_{l-1}}$  are the *weight matrices* and  $b^{(l)} \in \mathbb{R}^{N_l}$  are called *bias vectors*. The output  $\Phi_a(z; \theta)$  of the NN for an input  $z \in \mathbb{R}^{N_0}$  is then defined as  $\Phi_a(z; \theta) := \Phi^{(L)}(z; \theta)$ , where

$$\begin{aligned} \Phi^{(1)}(z; \theta) &= W^{(1)}z + b^{(1)}, \\ \hat{\Phi}^{(l)}(z; \theta) &= \rho(\Phi^{(l)}(z; \theta)), \quad l = 1, \dots, L-1, \quad \text{and} \\ \Phi^{(l+1)}(z; \theta) &= W^{(l+1)}\hat{\Phi}^{(l)}(z; \theta) + b^{(l+1)}, \quad l = 1, \dots, L-1, \end{aligned}$$

and  $\rho$  is applied component-wise. In the following the architecture is omitted in the notation as we view it as being fixed once and for all.

NNs seem suitable for solving PDEs because they are universal function approximators, see [17–19]. For a NN  $\Phi^\theta := \Phi(\cdot; \theta)$  to approximate the solution of a PDE, the parameters  $\theta$  must be determined, which is done in the training phase. Thereby, a tailored minimization problem is defined, with which the parameters are *learned*. In the regime of PINNs the function to be minimized involves the PDE (e.g. in classical form (2.1)), which is the reason for the name *physics-informed*.

With respect to the classical form of the PDE, a set of sample points  $\mathcal{S}_\Omega$  in  $\Omega$  are chosen and (2.1) is posed only for those points. This leads to the definition of the loss function

$$(2.3) \quad \mathcal{L}(\theta) := \sum_{x \in \mathcal{S}_\Omega} |(r_\Omega^\circ(\Phi^\theta))(x)|^2.$$

Often, an additional sampling is required for satisfying the boundary conditions. We shall assume that  $\Phi^\theta$  satisfies given boundary condition as this can be achieved with the aid of approximate distance functions, see [20].

Such classical PINNs have e.g. been investigated for a broad scope of linear and nonlinear PDEs, see e.g. [5, 21–25]. The main advantages of the method are its straightforward applicability and, due to the sampling of  $\mathcal{S}_\Omega$ , it results in a mesh-free approximation.

One can also replace the above loss function by terms stemming from a variational formulation of a given PDE, e.g. VPINNs. Again, as the specific form of the PINN is not relevant for our paper, we will not go into more details and only assume that  $\Phi^\theta$  gives some approximation for the solution of a given PDE.

## 3. ERROR-RESIDUAL RELATIONS FOR PDES

In this section, we recall the main facts on error-residual relations for PDEs, which is based upon the well-known Hilbert space theory of PDEs yielding well-posed formulations.

**3.1. Well-posedness.** Given a partial differential operator  $B$  (eventually starting from a classical version  $B^\circ$ ), we require Hilbert spaces  $\mathcal{W}$ ,  $\mathcal{Y}$  with norms  $\|\cdot\|_{\mathcal{X}}$  induced by inner products  $(\cdot, \cdot)_{\mathcal{X}}$ ,  $\mathcal{X} \in \{\mathcal{W}, \mathcal{Y}\}$ , such that the PDE

$$(3.1) \quad Bu = f$$

is *well-posed* for any appropriate right-hand side  $f$ , by which we mean that (3.1) admits a unique solution, which continuously depends on the data (typically the right-hand side  $f$ ). In order to ensure this, the domain  $\mathcal{W}$  and the range  $\mathcal{Y}'$  of the operator  $B$  have to be identified such that  $B \in \mathcal{L}_{\text{is}}(\mathcal{W}, \mathcal{Y}')^1$ , where  $\mathcal{Y}'$  is the topological dual space of  $\mathcal{Y}$  equipped with the operator norm

$$\|f\|_{\mathcal{Y}'} := \sup_{v \in \mathcal{Y}} \frac{f(v)}{\|v\|_{\mathcal{Y}}} = \sup_{v \in \mathcal{Y}} \frac{\langle f, v \rangle_{\mathcal{Y}}}{\|v\|_{\mathcal{Y}}},$$

i.e.,  $\langle \cdot, \cdot \rangle_{\mathcal{Y}} \equiv \langle \cdot, \cdot \rangle_{\mathcal{Y}' \times \mathcal{Y}}$  denotes the dual pairing. The reason why we choose the dual  $\mathcal{Y}'$  for the range of  $B$  lies in the fact that this easily allows one to relate the differential operator to a bilinear form

$$b : \mathcal{W} \times \mathcal{Y} \rightarrow \mathbb{R} \quad \text{via} \quad b(w, y) := \langle Bw, y \rangle_{\mathcal{Y}}, \quad w \in \mathcal{W}, y \in \mathcal{Y}.$$

If  $B \in \mathcal{L}_{\text{is}}(\mathcal{W}, \mathcal{Y}')$ , the operator is bijective, which ensures existence and uniqueness for all  $f \in \mathcal{Y}'$ . Moreover, the inverse is bounded, i.e.,

$$\|B^{-1}\|_{\mathcal{L}(\mathcal{Y}', \mathcal{W})} < \infty,$$

which will be relevant next.

Assume that we are given some approximation  $u^\delta$  of the (exact, but typically unknown) solution  $u \in \mathcal{W}$ , e.g. determined by some PINN. Then, we are interested in controlling the error  $\|u - u^\delta\|_{\mathcal{W}}$ . If  $B \in \mathcal{L}_{\text{is}}(\mathcal{W}, \mathcal{Y}')$ , one can bound the error by the dual norm of the *residual*  $r_B(u^\delta) := f - Bu^\delta \in \mathcal{Y}'$  as

$$(3.2) \quad \|B\|_{\mathcal{L}(\mathcal{W}, \mathcal{Y}')}^{-1} \cdot \|r_B(u^\delta)\|_{\mathcal{Y}'} \leq \|u - u^\delta\|_{\mathcal{W}} \leq \|B^{-1}\|_{\mathcal{L}(\mathcal{Y}', \mathcal{W})} \cdot \|r_B(u^\delta)\|_{\mathcal{Y}'}$$

The constants  $c_B := \|B\|_{\mathcal{L}(\mathcal{W}, \mathcal{Y}')}^{-1} > 0$  on the left and  $C_B := \|B^{-1}\|_{\mathcal{L}(\mathcal{Y}', \mathcal{W})} < \infty$  on the right of (3.2) are the (inverse of the) continuity and stability (inf-sup) constants, respectively. Then, (3.2) reads

$$(3.3) \quad c_B \|r_B(u^\delta)\|_{\mathcal{Y}'} \leq \|u - u^\delta\|_{\mathcal{W}} \leq C_B \|r_B(u^\delta)\|_{\mathcal{Y}'}, \quad \forall u^\delta \in \mathcal{W}.$$

Hence, we can bound the error from above and from below by the residual, if we

- either know or are able to compute or estimate the continuity and stability constants and
- are able to evaluate the dual norm of the residual, i.e.

$$\|r_B(u^\delta)\|_{\mathcal{Y}'} = \sup_{v \in \mathcal{Y}} \frac{\langle r_B(u^\delta), v \rangle_{\mathcal{Y}}}{\|v\|_{\mathcal{Y}}}.$$

However, the computation of the supremum is in general not possible.

---

<sup>1</sup>The space  $\mathcal{L}_{\text{is}}(\mathcal{W}, \mathcal{Y}')$  is the subspace of isomorphisms from  $\mathcal{L}(\mathcal{W}, \mathcal{Y}')$ , where  $(\mathcal{L}(\mathcal{W}, \mathcal{Y}'), \|\cdot\|_{\mathcal{L}(\mathcal{W}, \mathcal{Y}')} )$  denotes the space of continuous linear functions from  $\mathcal{W}$  to  $\mathcal{Y}'$ .

**3.2. PDEs on domains.** The above introduced abstract spaces  $\mathcal{W}$  and  $\mathcal{Y}$  are typically function spaces which are defined upon a physical domain  $\Omega \subset \mathbb{R}^d$ , on which the PDE is posed. Hence, we sometimes use the notations  $\mathcal{W}(\Omega)$  and  $\mathcal{Y}(\Omega)$ , also for domains different from the original  $\Omega$ . Boundary and/or initial conditions are incorporated into the definition of the operator  $B$ . It will be important later to keep track on the domain  $\Omega$ .

**Example 3.1** (Linear elliptic PDE). Let  $\Omega \subset \mathbb{R}^d$  be a Lipschitz domain and let  $\mathcal{W} = \mathcal{Y} = H_0^1(\Omega)$ . Given  $f \in H^{-1}(\Omega)$ , the problem of finding  $u \in H_0^1(\Omega)$  satisfying

$$\langle Bu, v \rangle_{H_0^1(\Omega)} := (A \nabla u, \nabla v)_{L_2(\Omega)} + (b \cdot \nabla u, v)_{L_2(\Omega)} + (c \cdot u, v)_{L_2(\Omega)} = f(v)$$

for all  $v \in H_0^1(\Omega)$  is well-posed, if  $A \in (L_\infty(\Omega))^{d \times d}$ ,  $b \in (L_\infty(\Omega))^d$ ,  $c \in L_\infty(\Omega)$  and

$$\nabla \cdot b \in L_2(\Omega), \quad c(x) - \frac{1}{2} \nabla \cdot b(x) \geq c_0 \quad \forall x \in \Omega \quad \text{a.e.}$$

as well as

$$\xi^T A(x) \xi \geq a_0 |\xi|^2, \quad \forall \xi \in \mathbb{R}^d \quad \forall x \in \Omega \quad \text{a.e.},$$

i.e.,  $A$  is s.p.d. In this case (3.3) holds with  $c = (\|A\|_\infty + s_{\text{PF}} \|b\|_\infty + s_{\text{PF}}^2 \|c\|_\infty)^{-1}$  and  $C = a_0^{-1}$ , whereby  $s_{\text{PF}}$  is the Poincaré constant for  $\Omega$ .  $\diamond$

**Example 3.2** (Space-time variational form of parabolic PDEs). Let the PDE operator  $A \in \mathcal{L}_{\text{is}}(W(\Omega), Y'(\Omega))$  be well-posed on some domain  $\Omega \subset \mathbb{R}^d$  for appropriate function spaces  $W(\Omega)$  and  $Y(\Omega)$ . Then, given  $f \in \mathcal{Y}' = L_2(I; Y'(\Omega)) := \{g : I \rightarrow Y'(\Omega) : \|g\|_{L_2(I; Y'(\Omega))}^2 := \int_I \|g(t)\|_{Y'(\Omega)}^2 dt < \infty\}$ , we seek a solution  $u \in \mathcal{W}$  (with  $\mathcal{W}$  to be defined) of the evolution problem  $Bu := \dot{u} + Au = f$  in  $\mathcal{Y}'$  and  $u(0) = 0$ . It is well-known that the Bochner space  $\mathcal{W} := \{w \in L_2(I; W(\Omega)) : \dot{w} \in L_2(I; W'(\Omega)), w(0) = 0\}$  equipped with the graph norm  $\|u\|_{\mathcal{W}}^2 := \|\partial_t u\|_{L_2(I, W'(\Omega))}^2 + \|u\|_{L_2(I, W(\Omega))}^2$  yields  $B \in \mathcal{L}_{\text{is}}(\mathcal{W}, \mathcal{Y}')$ , [26, 27]. This is known as the space-time variational formulation of parabolic PDEs, see also [28, 29]. If  $A$  is elliptic, one has  $W(\Omega) = Y(\Omega) = H_0^1(\Omega)$ .  $\diamond$

**3.3. Dual norm estimates.** We will now address the problem of finding a computable surrogate for the dual norm of the residual for well-posed PDE operator equations. To simplify the notation we consider general functionals  $f \in \mathcal{Y}'$  instead of the residual  $r_\Omega(u^\delta)$ . We want to calculate or estimate the dual norm of the functional  $f \in \mathcal{Y}'$ , i.e., we seek a feasible surrogate  $\eta(f)$  such that either

$$(3.4a) \quad \eta(f) = \|f\|_{\mathcal{Y}'}, \quad (\text{identity})$$

$$(3.4b) \quad \exists C, c > 0 : \quad c \eta(f) \leq \|f\|_{\mathcal{Y}'} \leq C \eta(f), \quad \text{or} \quad (\text{estimate})$$

$$(3.4c) \quad \exists C > 0 : \quad \|f\|_{\mathcal{Y}'} \leq C \eta(f) \quad (\text{bound})$$

holds. Ideally, we find  $\eta(f)$  such that identity (3.4a) is fulfilled, but this is typically not possible. Hence, one resorts to an estimate (3.4b), which ensures that  $\eta(f)$  encloses the desired quantity and  $\|f\|_{\mathcal{Y}'}$  is small if and only if  $\eta(f)$  is. If this is still not achievable, a bound (3.4c), if not too loose, guarantees at least that the desired quantity is below a threshold, if the bound is so.

By applying (3.4a) or (3.4b) to (3.3), the error is controlled by  $\eta$  as

$$c \cdot \eta(r_\Omega(u^\delta)) \leq \|u - u_\delta\|_{\mathcal{W}} \leq C \cdot \eta(r_\Omega(u^\delta)), \quad c, C > 0$$

or by using (3.4c) we have

$$\|u - u_\delta\|_{\mathcal{W}} \leq C \cdot \eta(r_\Omega(u^\delta)), \quad C > 0.$$

Notice that the constants  $c$  and  $C$  in the last two equations could be different to those of (3.3).

In the next section we shall describe how to find an efficient surrogate  $\eta$  for PINNs, such that one of the equations (3.4) is satisfied. It is clear that the structure of the underlying space  $\mathcal{Y}$  is crucial for the derivation.

**3.4. Riesz representation.** Since  $\mathcal{Y}$  is a Hilbert space, the Riesz Representation Theorem (see e.g. [30]) states that  $\eta(f)$  fulfilling (3.4a) is given by

$$\eta(f) := \|R_{\mathcal{Y}}^{-1}f\|_{\mathcal{Y}},$$

where  $R_{\mathcal{Y}} : \mathcal{Y} \rightarrow \mathcal{Y}'$  denotes the Riesz-operator defined through the equation  $(u, v)_{\mathcal{Y}} = \langle R_{\mathcal{Y}}u, v \rangle_{\mathcal{Y}'}$ ,  $u, v \in \mathcal{Y}$ , where  $(\cdot, \cdot)_{\mathcal{Y}}$  denotes the inner product in  $\mathcal{Y}$ . The Riesz representative  $\hat{f} := R_{\mathcal{Y}}^{-1}f \in \mathcal{Y}$  is found by solving the equation

$$(3.5) \quad (\hat{f}, v)_{\mathcal{Y}} = f(v), \quad \forall v \in \mathcal{Y}.$$

Since  $R_{\mathcal{Y}}$  is isometric we have  $\eta(f) = \|f\|_{\mathcal{Y}'}$  and thus (3.4a). Usually, evaluating  $\|\cdot\|_{\mathcal{Y}}$  is much easier than evaluating  $\|\cdot\|_{\mathcal{Y}'}$ . Unfortunately, calculating the Riesz representative with (3.5) is still unfeasible because the space  $\mathcal{Y}$  is in almost all cases infinite-dimensional. Therefore,  $\mathcal{Y}$  is replaced by a sufficiently high but finite-dimensional subspace  $\mathcal{Y}^{\delta} \subset \mathcal{Y}$ , e.g., a finite element space. The Riesz representative  $\hat{f} \in \mathcal{Y}$  is then approximated by  $\hat{f}^{\delta} \in \mathcal{Y}^{\delta}$ , which is the solution of

$$(3.6) \quad (\hat{f}^{\delta}, v^{\delta})_{\mathcal{Y}} = f(v^{\delta}), \quad \forall v^{\delta} \in \mathcal{Y}^{\delta}.$$

**Remark 3.3.** *If  $\mathcal{Y}$  is not a Hilbert, but only a Banach space, the Riesz Representation Theorem is not applicable. However, one way out is to use wavelet methods to directly bound the dual norm  $\|f\|_{\mathcal{Y}'}$  as proposed in [9].*

With an increasing dimension of  $\mathcal{Y}^{\delta}$  we can at least hope to have convergence of  $\hat{f}^{\delta}$  to  $\hat{f}$  in  $\mathcal{Y}$  and therefore convergence of  $\|\hat{f}^{\delta}\|_{\mathcal{Y}}$  to  $\|\hat{f}\|_{\mathcal{Y}}$ . The drawback of this approach is that, in the case of finite elements, the space  $\mathcal{Y}^{\delta}$  requires a discretization of the underlying domain  $\Omega$ .

#### 4. CERTIFICATION VIA EXTENSIONS AND RESTRICTIONS

Now we are in position to describe the proposed approach towards deriving efficiently computable lower and upper bounds for the error  $\|u - u^{\theta}\|_{\mathcal{W}}$  of a PINN  $u^{\theta}$  for approximating the solution  $u$  of a PDE operator equation  $Bu = f$ . The idea is to use the residual  $r^{\theta} := f - Bu^{\theta}$  on different domains, i.e.,

$$\bigcirc \subset \Omega \subset \square \subset \mathbb{R}^d,$$

where we shall use  $\bigcirc$  to derive a lower and  $\square$  for an upper bound. This approach has a couple of consequences which we will address next:

- We need to compute the Riesz representation of  $r_{\theta}$  by solving (3.6) replacing  $f$  by  $r^{\theta}$ . Hence, we need to compute  $r^{\theta}(v^{\delta})$  for appropriate test functions  $v^{\delta}$  on the respective domain. This typically amounts for computing inner products, i.e., integrals. If the PINN gives pointwise approximations, we use quadrature (e.g. by choosing Gauss-Lobatto points), for a variational PINN, we would precompute the inner products of the basis functions and then determine the linear combinations.
- We need to restrict and extend  $r^{\theta}$  to  $\bigcirc$  and  $\square$  in an appropriate manner.

- We have to choose  $\circ$  and  $\square$  in such a way that (i) the residuals on these domains allow for sharp error bounds and (ii) the computations are very efficient, which typically means that the geometries of  $\circ$  and  $\square$  need to be “simple”, e.g. a hypersphere or -cube. Then, standard discretizations and fast solvers such as geometric full multigrid or spectral methods are available.

We need to fix some notation. The original PDE operator equation  $Bu = f$  is posed in  $\mathcal{Y}'(\Omega)$  for  $B \in \mathcal{L}_{\text{is}}(\mathcal{W}(\Omega), \mathcal{Y}'(\Omega))$ , the residual  $r^\theta$  is an element of  $\mathcal{Y}'(\Omega)$ , its Riesz representation  $\hat{r}_\Omega^\theta$  on  $\Omega$  is determined by solving a sufficiently detailed discretization of the problem finding

$$(4.1) \quad \hat{r}_\Omega^\theta \in \mathcal{Y}(\Omega) : \quad (\hat{r}_\Omega^\theta, v)_{\mathcal{Y}(\Omega)} = r_\Omega^\theta(v) \quad \forall v \in \mathcal{Y}(\Omega).$$

**4.1. Extension and restriction for primal and dual spaces.** One might think that we could just consider the problem (4.1) by changing  $\Omega$  to  $\circ$  and  $\square$ , respectively. This, however, does not match our goals. Recall that  $\mathcal{Y}(\Omega)$  is typically a function space, e.g.  $H_0^1(\Omega)$ . Just changing  $\Omega$  to  $\square$  would give rise to  $H_0^1(\square)$ . However, the restriction of a function in  $H_0^1(\square)$  to  $\Omega$  is in general *not* in  $H_0^1(\Omega)$ . Moreover, depending on the geometry of  $\Omega$ , an extension might be a delicate issue. Finally, we cannot hope to control the norms of the residual on  $\Omega$  by those on  $\circ$  and  $\square$ . To overcome this difficulty, we propose the following recipe:

1. Choose a space  $\mathcal{Z}(\square)$ , which contains all extensions of  $\mathcal{Y}(\Omega)$  by zero and which allows for fast solvers. One may think of  $H_0^1(\square)$  or  $H_{\text{per}}^1(\square)$ .
2. Identify a subspace  $\mathcal{U}(\square) \subseteq \mathcal{Z}(\square)$ , which is isomorphic to  $\mathcal{Y}(\Omega)$ , i.e.,  $\mathcal{U}(\square) \cong \mathcal{Z}(\square)$ .

We are going to formalize this idea in the following assumption.

**Assumption 4.1.** *Let  $\Omega \subset \square \subset \mathbb{R}^d$  be Lipschitz domains, and let  $\mathcal{Y}(\Omega)$  and  $\mathcal{Z}(\square)$  be given function spaces.*

- (a) *Then, assume that there exists a subspace  $\mathcal{U}(\square) \subset \mathcal{Z}(\square)$  (with the same norm  $\|\cdot\|_{\mathcal{Z}(\square)}$  as in  $\mathcal{Z}(\square)$ ), which is isomorphic to  $\mathcal{Y}(\Omega)$ .*
- (b) *The isomorphism is denoted by  $E_{\Omega \rightarrow \square} \in \mathcal{L}_{\text{is}}(\mathcal{Y}(\Omega), \mathcal{U}(\square))$ .*
- (c) *We denote the continuous inverse operator of  $E_{\Omega \rightarrow \square}$  by  $R_{\Omega \leftarrow \square} := E_{\Omega \rightarrow \square}^{-1}$ .*  $\diamond$

Although the assumption requiring an isomorphism seems to be quite strong, we will see that for a large class of spaces we can in fact construct such an isomorphism. The names  $E_{\Omega \rightarrow \square}$  and  $R_{\Omega \leftarrow \square}$  are chosen to emphasize that the operators are often *extension* and *restriction*, at least in our examples described in Section 5.

We note a simple immediate consequence of Assumption 4.1.

**Corollary 4.2.** *If Assumption 4.1 holds, then*

$$c_\square \|v\|_{\mathcal{Y}(\Omega)} \leq \|E_{\Omega \rightarrow \square} v\|_{\mathcal{Z}(\square)} \leq C_\square \|v\|_{\mathcal{Y}(\Omega)}, \quad \forall v \in \mathcal{Y}(\Omega),$$

where  $c_\square := \|R_{\Omega \leftarrow \square}\|_{\mathcal{L}(\mathcal{U}(\square), \mathcal{Y}(\Omega))}^{-1}$  and  $C_\square := \|E_{\Omega \rightarrow \square}\|_{\mathcal{L}(\mathcal{Y}(\Omega), \mathcal{U}(\square))}$ .  $\square$

With the operator  $E_{\Omega \rightarrow \square}$ , we have the desired connection between the primal spaces  $\mathcal{Y}(\Omega)$  and  $\mathcal{Z}(\square)$ . We need such a relation also for the dual spaces. For that, we consider the adjoint operators  $E'_{\Omega \leftarrow \square} \in \mathcal{L}_{\text{is}}(\mathcal{U}'(\square), \mathcal{Y}'(\Omega))$  of  $E_{\Omega \rightarrow \square}$  and  $R'_{\Omega \rightarrow \square} \in \mathcal{L}_{\text{is}}(\mathcal{Y}'(\Omega), \mathcal{U}'(\square))$  of the inverse of  $E_{\Omega \rightarrow \square}$ . By definition of adjoint operators, we



have

$$\begin{aligned}\langle E'_{\Omega \leftarrow \square} f_{\square}, v \rangle_{\mathcal{Y}(\Omega)} &= \langle f_{\square}, E_{\Omega \rightarrow \square} v \rangle_{\mathcal{U}(\square)}, & \forall v \in \mathcal{Y}(\Omega), \forall f_{\square} \in \mathcal{U}'(\square) \quad \text{and} \\ \langle R'_{\Omega \rightarrow \square} f_{\Omega}, w \rangle_{\mathcal{U}(\square)} &= \langle f_{\Omega}, R_{\Omega \leftarrow \square} w \rangle_{\mathcal{Y}(\Omega)}, & \forall w \in \mathcal{U}(\square), \forall f_{\Omega} \in \mathcal{Y}'(\Omega).\end{aligned}$$

Furthermore, for the norm there holds  $\|E_{\Omega \rightarrow \square}\|_{\mathcal{L}(\mathcal{Y}(\Omega), \mathcal{U}(\square))} = \|E'_{\Omega \leftarrow \square}\|_{\mathcal{L}(\mathcal{U}'(\square), \mathcal{Y}'(\Omega))}$  and  $\|R_{\Omega \leftarrow \square}\|_{\mathcal{L}(\mathcal{U}(\square), \mathcal{Y}(\Omega))} = \|R'_{\Omega \rightarrow \square}\|_{\mathcal{L}(\mathcal{Y}'(\Omega), \mathcal{U}'(\square))}$ . Note that the dual operators  $R'_{\Omega \rightarrow \square}$  and  $E'_{\Omega \leftarrow \square}$  are changing the roles of extension and restriction. In fact,  $R'_{\Omega \rightarrow \square}$  is an extension operator for functionals defined on  $\mathcal{Y}(\Omega)$  onto those on  $\mathcal{U}(\square)$ . Apparently, this requires the dual space  $\mathcal{U}'(\square)$  of  $\mathcal{U}(\square)$ , whose norm is given by

$$\|r\|_{\mathcal{U}'(\square)} = \sup_{u \in \mathcal{U}(\square)} \frac{r(u)}{\|u\|_{\mathcal{Z}(\square)}},$$

which is in general smaller than  $\|r\|_{\mathcal{Z}'(\square)}$  if  $\mathcal{U}(\square) \subsetneq \mathcal{Z}(\square)$ . With this norm, we have the following estimate.

**Lemma 4.3.** *Let Assumption 4.1 hold, then*

$$(4.2) \quad c_{\square} \|R'_{\Omega \rightarrow \square} f_{\Omega}\|_{\mathcal{U}'(\square)} \leq \|f_{\Omega}\|_{\mathcal{Y}'(\Omega)} \leq C_{\square} \|R'_{\Omega \rightarrow \square} f_{\Omega}\|_{\mathcal{U}'(\square)} \quad \forall f_{\Omega} \in \mathcal{Y}'(\Omega)$$

with the constants  $0 < c_{\square} \leq C_{\square} < \infty$  defined in Corollary 4.2.

*Proof.* The lower bound is the continuity of  $R'_{\Omega \rightarrow \square}$ , i.e.

$$\|R'_{\Omega \rightarrow \square} f_{\Omega}\|_{\mathcal{U}'(\square)} \leq \|R'_{\Omega \rightarrow \square}\|_{\mathcal{L}(\mathcal{Y}'(\Omega), \mathcal{U}'(\square))} \|f_{\Omega}\|_{\mathcal{Y}'(\Omega)} \leq \frac{1}{c_{\square}} \|f_{\Omega}\|_{\mathcal{Y}'(\Omega)}.$$

The upper bound follows from the continuity of  $E'_{\Omega \leftarrow \square}$  and the fact that  $\text{id}_{\mathcal{Y}'(\Omega)} = (\text{id}_{\mathcal{Y}(\Omega)})' = (R_{\Omega \leftarrow \square} \circ E_{\Omega \rightarrow \square})' = (E'_{\Omega \leftarrow \square} \circ R'_{\Omega \rightarrow \square})'$ , which concludes the proof.  $\square$

The estimates in Lemma 4.3 seem to give us the desired upper and lower bounds. However, they involve the norm in  $\mathcal{U}'(\square)$ , i.e., we would need the space  $\mathcal{U}(\square)$ , which turns out to be inappropriate as the following example shows.

**Example 4.4.** Let  $\mathcal{Y}(\Omega) = H_0^1(\Omega)$  and  $\mathcal{Z}(\square) = H_0^1(\square)$ . We are searching for a subspace  $\mathcal{U}(\square) \subset \mathcal{Z}(\square)$ , which is isomorphic to  $\mathcal{Y}(\Omega)$ . Apparently, the extension by zero of an element of  $H_0^1(\Omega)$  is in  $H_0^1(\square)$ , and the restriction of an element in  $H_0^1(\square)$  having zero trace on  $\partial\Omega$  is in  $H_0^1(\Omega)$ . Hence, we could choose  $\mathcal{U}(\square)$  consisting of all zero extensions of  $H_0^1(\Omega)$ -functions. To compute those functions, would however require a discretization of  $\Omega$ , which we wanted to avoid.  $\diamond$

This latter example shows that we need to be careful with the definition of the operators  $E_{\Omega \rightarrow \square}$  yielding  $\mathcal{Z}(\square)$  and the subspace  $\mathcal{U}(\square)$ . We want to do all computations on  $\mathcal{Z}(\square)$ , which means that we need a norm-preserving extension from  $f_{\Omega} \in \mathcal{Y}'(\Omega)$  via  $R'_{\Omega \rightarrow \square} f_{\Omega} \in \mathcal{U}'(\square)$  to  $\mathcal{Z}'(\square)$ . To this end, we suggest the norm-preserving Hahn-Banach Extension Theorem (see e.g. [31, Sec. 9.1.2, Th.1]), ensuring the existence of extensions  $f_{\square}^{\text{HB}} \in \mathcal{Z}'(\square)$  of  $R'_{\Omega \rightarrow \square} f_{\Omega} \in \mathcal{U}'(\square)$  with

$$\|R'_{\Omega \rightarrow \square} f_{\Omega}\|_{\mathcal{U}'(\square)} = \|f_{\square}^{\text{HB}}\|_{\mathcal{Z}'(\square)}.$$

For all other extensions of  $R'_{\Omega \rightarrow \square} f_{\Omega}$ , the lower bound from Lemma 4.3 will be lost. Unfortunately, the proof of the Hahn-Banach Extension Theorem is non-constructive, i.e., the Hahn-Banach extension  $f_{\square}^{\text{HB}}$  is not known in general. Thus, we will describe the computation of extensions of  $R'_{\Omega \rightarrow \square} f_{\Omega}$  in §4.3 below.

**4.2. A lower bound.** For deriving a lower bound, we suggest to use an additional domain  $\circ \subset \Omega$  and a corresponding function space  $\mathcal{X}(\circ)$  in such a way that Assumption 4.1 holds for the spaces  $\mathcal{X}(\circ)$  and  $\mathcal{Y}(\Omega)$  replacing  $\mathcal{Y}(\Omega)$  and  $\mathcal{Z}(\square)$ . Then, there exists a subspace  $\mathcal{V}(\Omega) \subset \mathcal{Y}(\Omega)$ , which is isomorphic to  $\mathcal{X}(\circ)$ . We denote the corresponding extension isomorphism and its inverse (the restriction) by  $E_{\circ \rightarrow \Omega}$  and  $R_{\circ \leftarrow \Omega}$ . Moreover, by switching the roles of  $R'_{\circ \rightarrow \Omega}$  and  $E'_{\circ \leftarrow \Omega}$  we get the following bound.

**Lemma 4.5.** *Let Assumption 4.1 hold, such that there exists an operator  $E \in \mathcal{L}_{is}(\mathcal{X}(\circ), \mathcal{V}(\Omega))$ . Then,*

$$(4.3) \quad \frac{1}{C_{\circ}} \|E'_{\circ \leftarrow \Omega} f_{\Omega}\|_{\mathcal{X}'(\circ)} \leq \|f_{\Omega}\|_{\mathcal{V}'(\Omega)} \leq c_{\circ} \|E'_{\circ \leftarrow \Omega} f_{\Omega}\|_{\mathcal{X}'(\circ)} \quad \forall f_{\Omega} \in \mathcal{V}'(\Omega)$$

where  $c_{\circ} := \|R_{\circ \leftarrow \Omega}\|_{\mathcal{L}(\mathcal{V}(\Omega), \mathcal{X}(\circ))}^{-1}$  and  $C_{\circ} := \|E_{\circ \rightarrow \Omega}\|_{\mathcal{L}(\mathcal{X}(\circ), \mathcal{V}(\Omega))}$ .

*Proof.* The lower bound follows from the continuity of  $E'_{\circ \leftarrow \Omega}$  and the upper bound is derived using  $\text{id}_{\mathcal{X}(\circ)} = R_{\circ \leftarrow \Omega} \circ E_{\circ \rightarrow \Omega}$  and the continuity of  $R_{\circ \leftarrow \Omega}$ .  $\square$

Now, we can put all pieces together and formulate the main result of this section. To this end, it is convenient to define for spaces  $\mathcal{X} \subset \mathcal{Y}$  the *set of all extensions* of a given functional  $f \in \mathcal{X}'$  as

$$\mathcal{E}(f; \mathcal{Y}') := \{\tilde{f} \in \mathcal{Y}' : \tilde{f} \equiv f \text{ on } \mathcal{X}\}.$$

With that at hand, we combine Lemma 4.3 and Lemma 4.5.

**Theorem 4.6.** *Let  $\circ \subset \Omega \subset \square$  and  $f_{\Omega} \in \mathcal{V}'(\Omega)$  be given. Furthermore, let  $E_{\Omega \rightarrow \square}$ ,  $R_{\Omega \leftarrow \square}$  and  $E_{\circ \rightarrow \Omega}$ ,  $R_{\circ \leftarrow \Omega}$  be the operators from Lemma 4.3 and from Lemma 4.5, respectively. Then we have*

$$\frac{1}{C_{\circ}} \|f_{\circ}\|_{\mathcal{X}'(\circ)} \leq \|f_{\Omega}\|_{\mathcal{V}'(\Omega)} \leq C_{\square} \|f_{\square}\|_{\mathcal{Z}'(\square)},$$

for all  $f_{\square} \in \mathcal{E}(R'_{\Omega \rightarrow \square} f_{\Omega}; \mathcal{Z}'(\square))$  and  $f_{\circ} := E'_{\circ \leftarrow \Omega}(f_{\Omega}|_{\mathcal{V}(\Omega)})$ , where  $f_{\Omega}|_{\mathcal{V}(\Omega)}$  denotes the restriction of  $f_{\Omega} : \mathcal{Y}(\Omega) \rightarrow \mathbb{R}$  to  $\mathcal{V}(\Omega) \subset \mathcal{Y}(\Omega)$ .

*Proof.* To derive the upper bound, we first use Lemma 4.3, which yields  $\|f_{\Omega}\|_{\mathcal{V}'(\Omega)} \leq C_{\square} \|R'_{\Omega \rightarrow \square} f_{\Omega}\|_{\mathcal{U}'(\square)}$ . Next, the Hahn-Banach Extension Theorem ensures the existence of an extension  $f_{\square}^{\text{HB}} \in \mathcal{Z}'(\square)$  of  $R'_{\Omega \rightarrow \square} f_{\Omega} \in \mathcal{U}'(\square)$  to  $\mathcal{Z}'(\square)$  with the identity  $\|R'_{\Omega \rightarrow \square} f_{\Omega}\|_{\mathcal{U}'(\square)} = \|f_{\square}^{\text{HB}}\|_{\mathcal{Z}'(\square)}$  and all other extensions have larger norms, which proves the upper bound. For the lower bound, note that  $\mathcal{V}'(\Omega) \subset \mathcal{V}'(\Omega)$ , so that  $\|f_{\Omega}|_{\mathcal{V}(\Omega)}\|_{\mathcal{V}'(\Omega)} \leq \|f_{\Omega}\|_{\mathcal{V}'(\Omega)}$  (again by the Hahn-Banach theorem). Finally, the lower bound in Lemma 4.5 applied to  $f_{\Omega}|_{\mathcal{V}(\Omega)} \in \mathcal{V}'(\Omega)$  completes the proof.  $\square$

**4.3. Constructing an extension.** The main building blocks of the above theory are the extension isomorphism  $E_{\circ \rightarrow \Omega}$  and  $E_{\Omega \rightarrow \square}$ , their duals and their inverses. Of course, the extensions depend on the geometry of  $\Omega$  and the specific form of the spaces  $\mathcal{Y}(\Omega)$  and  $\mathcal{Z}(\square)$ , which in turn are determined by the underlying PDE. We are going to detail two relevant cases.

**4.3.1. Sobolev Spaces with zero trace.** Let  $\Omega \subset \mathbb{R}^d$  and let  $\mathcal{Y}(\Omega) = W_0^{m,p}(\Omega)$  be the Sobolev spaces of order  $m \in \mathbb{N}$  in  $L_p(\Omega)$  for  $1 \leq p \leq \infty$ . A *zero extension*  $\tilde{u}$  of  $u \in W_0^{m,p}(\Omega)$  is defined as

$$\tilde{u}(x) := \begin{cases} u(x), & x \in \Omega, \\ 0, & x \in \Omega^c := \mathbb{R}^d \setminus \Omega. \end{cases}$$

**Proposition 4.7** ([32, Lemma 3.27]). *Let  $u \in W_0^{m,p}(\Omega)$ . If  $|\alpha| \leq m$ , then  $D^\alpha \tilde{u} = \widetilde{D^\alpha u}$  in the distributional sense in  $\mathbb{R}^n$ , i.e.,  $\tilde{u} \in W^{m,p}(\mathbb{R}^n)$ .*  $\square$

Studying the proof of [32, Lemma 3.27], we note that there are no assumptions on the domain  $\Omega$ . In the following we denote the dual spaces of  $W_0^{m,p}(\Omega)$  by  $W_0^{-m,q}(\Omega) := (W_0^{m,p}(\Omega))'$  where  $\frac{1}{p} + \frac{1}{q} = 1$ .

Let  $u \in \mathcal{Y}(\Omega) := W_0^{m,p}(\Omega)$  for some  $\Omega \subset \mathbb{R}^d$ ,  $\tilde{u}$  be its zero extension to  $\mathbb{R}^d$  and let  $\tilde{u}|_\square$  be the restriction to  $\square \supset \Omega$ . Then,  $\tilde{u}|_\square \in W_0^{m,p}(\square)$  and we define

$$(4.4) \quad E_{\Omega \rightarrow \square} : W_0^{m,p}(\Omega) \rightarrow W_0^{m,p}(\square) \quad \text{by} \quad u \mapsto E_{\Omega \rightarrow \square} u := \tilde{u}|_\square,$$

which is a linear operator. Setting

$$(4.5) \quad \mathcal{U}(\square) := E_{\Omega \rightarrow \square}(W_0^{m,p}(\Omega)) \subsetneq \mathcal{Z}(\square) = W_0^{m,p}(\square),$$

i.e., the range of  $E_{\Omega \rightarrow \square}$ , Proposition 4.7 ensures that  $E_{\Omega \rightarrow \square} : W_0^{m,p}(\Omega) \rightarrow \mathcal{U}(\square)$  is an isometry, i.e.,

$$(4.6) \quad C_\square = \|E_{\Omega \rightarrow \square}\|_{\mathcal{L}(\mathcal{Y}(\Omega), \mathcal{U}(\square))} = 1.$$

Hence, the operator is continuous and bounded from below. By [33, Lemma 2.8], this is equivalent to  $E_{\Omega \rightarrow \square}$  being an isomorphism. The restriction  $R_{\Omega \leftarrow \square} : \mathcal{U}(\square) \rightarrow W_0^{m,p}(\Omega)$  is the inverse operator and we get  $c_\square = \|R_{\Omega \leftarrow \square}\|_{\mathcal{L}(\mathcal{Y}(\Omega), \mathcal{U}(\square))}^{-1} = 1$ . Note, that the constants in Corollary 4.2 are in fact unity here, which is due to the zero trace in combination with zero extension.

We can proceed in an analogous manner for  $\circ \subset \Omega$ ,  $\mathcal{X}(\circ) := W_0^{m,p}(\circ)$  and get an isomorphism  $E_{\circ \rightarrow \Omega} : W_0^{m,p}(\circ) \rightarrow \mathcal{V}(\Omega)$  defined as  $E_{\circ \rightarrow \Omega} u := \tilde{u}|_\Omega$  for

$$(4.7) \quad \mathcal{V}(\Omega) := E_{\circ \rightarrow \Omega}(W_0^{m,p}(\circ)) \subsetneq \mathcal{Y}(\Omega).$$

Again, we obtain isometries, i.e., the involved constants are unity. Thus, Theorem 4.6 implies the following statement.

**Corollary 4.8.** *Let  $\circ \subset \Omega \subset \square \subset \mathbb{R}^d$ ,  $\mathcal{X}(\circ) := W_0^{m,p}(\circ)$ ,  $\mathcal{Y}(\Omega) := W_0^{m,p}(\Omega)$  and  $\mathcal{Z}(\square) := W_0^{m,p}(\square)$  for  $m \in \mathbb{N}$  and  $1 \leq p \leq \infty$ . Let  $E_{\circ \rightarrow \Omega}$ ,  $E_{\Omega \rightarrow \square}$  be defined as above and  $R_{\circ \leftarrow \Omega}$ ,  $R_{\Omega \leftarrow \square}$  being their inverses. Then,*

$$(4.8) \quad \|f_\circ\|_{W_0^{-m,q}(\circ)} \leq \|f_\Omega\|_{W_0^{-m,q}(\Omega)} \leq \|f_\square\|_{W_0^{-m,q}(\square)}$$

for all  $f_\square \in \mathcal{E}(R'_{\Omega \rightarrow \square} f_\Omega; W_0^{-m,q}(\square))$  and  $f_\circ := E'_{\circ \leftarrow \Omega}(f_\Omega|_{\mathcal{V}(\Omega)})$  with  $\mathcal{V}(\Omega)$  defined in (4.7).  $\square$

**4.3.2. Bochner spaces.** We are now going to consider instationary parabolic problems involving space and time as already introduced in Example 3.2 for  $Y(\Omega) := W_0^{m,p}(\Omega)$ . We perform the embedding strategy only w.r.t. the space variable and set

$$\mathcal{X}(\circ) := L_2(I; W_0^{m,p}(\circ)), \quad \mathcal{Y}(\Omega) := L_2(I; W_0^{m,p}(\Omega)), \quad \mathcal{Z}(\square) := L_2(I; W_0^{m,p}(\square)),$$

for  $\circ \subset \Omega \subset \square \subset \mathbb{R}^d$ . Hence, we can reuse the findings of the previous §4.3.1. Using  $E_{\Omega \rightarrow \square}$  defined in (4.4) and  $U(\square) := E_{\Omega \rightarrow \square}(W_0^{m,p}(\Omega))$  as in (4.5), we define a space-time extension operator

$$E_{I \times \Omega \rightarrow I \times \square} : \mathcal{Y}(\Omega) = L_2(I; Y(\Omega)) \rightarrow L_2(I; U(\square)) =: \mathcal{U}(\square),$$

and

$$(4.9) \quad (E_{I \times \Omega \rightarrow I \times \square} v)(t) := E_{\Omega \rightarrow \square}(v(t)), \quad t \in I \text{ a.e.}, \quad v \in \mathcal{Y}(\Omega).$$

With this definition, the following result is immediate.

**Proposition 4.9.** *Let  $E_{\Omega \rightarrow \square} \in \mathcal{L}_{is}(Y(\Omega), U(\square))$ . Then, for  $E_{I \times \Omega \rightarrow I \times \square}$  defined as in (4.9), we have  $E_{I \times \Omega \rightarrow I \times \square} \in \mathcal{L}_{is}(L_2(I; Y(\Omega)), L_2(I; U(\square)))$ .*

*Proof.* By Corollary 4.2, we have that the function  $t \mapsto \|E_{\Omega \rightarrow \square}(v(t))\|_{Z(\square)}$ ,  $Z(\square) := W^{m,p}(\square)$ , is upper-bounded by the function  $t \mapsto C_{\square} \|(v(t))\|_{Y(\Omega)}$  and lower-bounded by the function  $t \mapsto \frac{1}{c_{\square}} \|(v(t))\|_{Y(\Omega)}$ . Thus,  $E_{I \times \Omega \rightarrow I \times \square} v \in L_2(I; U(\square))$  and the operator  $E_{I \times \Omega \rightarrow I \times \square}$  is continuous as well as bounded from below. Using again [33, Lemma 2.8], it remains to show that the range of  $E_{I \times \Omega \rightarrow I \times \square}$  is  $L_2(I; U(\square))$ . Given  $v \in L_2(I; U(\square))$ , define  $w \in L_2(I; Y(\Omega))$  by  $w(t) := R_{\Omega \leftarrow \square}(v(t))$  for almost all  $t \in I$ . With that we have  $E_{I \times \Omega \rightarrow I \times \square} w = v$ , which completes the proof.  $\square$

The inverse operator  $E_{I \times \Omega \rightarrow I \times \square}^{-1}$  is denoted by  $R_{I \times \Omega \leftarrow I \times \square}$ . Finally, we define  $E_{I \times \square \rightarrow I \times \Omega}$  and  $R_{I \times \square \leftarrow I \times \Omega}$  using the operators  $E_{\square \rightarrow \Omega}$ ,  $R_{\square \leftarrow \Omega}$  from Corollary 4.8, i.e.,  $(E_{I \times \square \rightarrow I \times \Omega} v)(t) := E_{\square \rightarrow \Omega}(v(t))$  and  $R_{I \times \square \leftarrow I \times \Omega} := E_{I \times \square \rightarrow I \times \Omega}^{-1}$ . Then, we can put everything together and obtain.

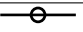




**Corollary 4.10.** *With  $\mathcal{X}(\circ)$ ,  $\mathcal{Y}(\Omega)$ ,  $\mathcal{Z}(\square)$  and the above operators, we have for all  $f_{\square} \in \mathcal{E}(R'_{I \times \Omega \rightarrow I \times \square} f_{\Omega}; L_2(I, W_0^{-m,q}(\square)))$*

$$(4.10) \quad \|f_{\square}\|_{L_2(I, W_0^{-m,q}(\square))} \leq \|f_{\Omega}\|_{L_2(I, W_0^{-m,q}(\Omega))} \leq \|f_{\square}\|_{L_2(I, W_0^{-m,q}(\square))},$$

setting  $f_{\square} := E'_{I \times \square \leftarrow I \times \Omega}(f_{\Omega}|_{L_2(I, \mathcal{V}'(\Omega))})$ .  $\square$

## 5. NUMERICAL EXPERIMENTS

We investigate the quantitative performance of the proposed error estimators for linear elliptic and parabolic PDEs. In order to do so, we compare the quantities listed in the following table.

legend	computation done by	
	$\mathcal{W}$ -error on $\Omega$	high-fidelity FE computation
	lower bound on $\Omega$	high-fidelity Riesz representation
	upper bound on $\Omega$	high-fidelity Riesz representation
	lower bound on $\square$	efficient error estimator
	upper bound on $\square$	efficient error estimator

The “true”  $\mathcal{W}$ -error (black) is computed by comparing the PINN-solution with a high-fidelity finite element reference solution. The upper and lower bounds in  $\Omega$  (blue lines) are determined by using the Riesz representation w.r.t. a fine discretization of the PDE on the domain  $\Omega$  and computing the dual norm of the residual by determining the primal norm of the Riesz representation. For all presented examples, we derive analytical estimates for the involved constants. Of course, this could also be replaced by solving corresponding generalized eigenvalue problems. These “Riesz estimates” on  $\Omega$  are used as a reference only, as those bounds require high computational cost (in that case, one could replace a PINN by the detailed FE simulation). It is clear that our error estimates cannot be better than the Riesz bounds on  $\Omega$ .

In order to compute our error estimator (orange), we need to solve the PDE on  $\square$  and  $\square$ . Hence, we choose these domains in such a way that their geometry is rather simple, e.g. a circle or a rectangle allowing for highly efficient tensorproduct discretizations in spherical and canonical coordinates, respectively. For those, we used highly efficient and accurate spectral methods, [34]. All experiments have

been carried out in Python with FEniCSx [35] and PyTorch [36]. Our code can be found on a `git` repository, [37].

As mentioned already above, possible scenarios for PINNs include parametric PDEs (PPDEs) and/or PDEs on (spatial) domains with complicated geometries. This also guides our numerical experiments. Denoting by  $\mathcal{P} \subset \mathbb{R}^P$ ,  $P \in \mathbb{N}$ , a compact parameter set, we denote by  $u_\mu^\delta$  the high-fidelity (but expensive) numerical solution of the PPDE (e.g. by finite elements). Then, we trained a PINN  $\Phi^\theta(\cdot; \mu)$  to approximate the solution maps  $\mu \mapsto u_\mu$ , where  $u_\mu$  is the exact (classical, i.e., pointwise) solution<sup>2</sup> of the PPDE on the domain  $\Omega$ . For our experiments, we trained the PINN using the mean-square loss function

$$\mathcal{L}(\theta) := \sum_{\mu \in \mathcal{S}_\mathcal{P}} \sum_{x \in \mathcal{S}_\Omega} |u_\mu^\delta(x) - \Phi^\theta(x; \mu)|^2,$$

where we used finite training data sets  $\mathcal{S}_\mathcal{P} \subset \mathcal{P}$  for the parameter and  $\mathcal{S}_\Omega \subset \Omega$  for the physical variable (which could also be space and time for parabolic problems). However, we stress once more the fact that our subsequent error estimation is independent on the specific loss function and training process.

**5.1. Linear parameter-dependent diffusion problem.** We start by a problem in space only, i.e., an elliptic problem involving parameters posed on a “complicated” domain  $\Omega \subset \mathbb{R}^d$  being the nonconvex saw-blade-like domain shown in Figure 1. The subdomain  $\Omega_1$  consists of the saw teeth and  $\Omega_2 := \Omega \setminus \Omega_1$  is a rectangle. In such a setting, the existence of a classical solution cannot be expected and a finite element solution will require to resolve the geometry of the domain.

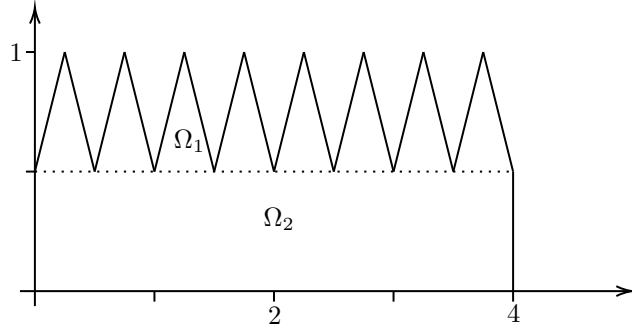


FIGURE 1. Saw-blade domain  $\Omega = \Omega_1 \cup \Omega_2$  with the partition for the diffusion coefficients. The saw teeth are made of different material than the saw blade.

The variational form of the PPDE uses the trial and test space  $\mathcal{W} = \mathcal{Y} = H_0^1(\Omega)$  yielding a Galerkin discretization and amounts finding  $u_\mu \in H_0^1(\Omega)$  such that

$$\langle r_\Omega(u_\mu), v \rangle_{H_0^1(\Omega)} := (A_\mu \nabla u_\mu, \nabla v)_{L_2(\Omega)} - (1, v)_{L_2(\Omega)} = 0 \quad \forall v \in H_0^1(\Omega),$$

where the parameter-dependent diffusion matrix is given by

$$A(x; \mu) := [\mu_1 \chi_{\Omega_1}(x) + \mu_2 \chi_{\Omega_2}(x)] \begin{pmatrix} 1 & 0 \\ 0 & 2 \end{pmatrix},$$

The diffusion is parameterized ranging in  $\mathcal{P} := [1/10, 1] \times [5/100, 1/10] \subset \mathbb{R}^2$ ,  $P = 2$ .

<sup>2</sup>Existence and uniqueness of such a solution is *not* clear!

The training set  $\mathcal{S}_{\mathcal{P}} \subset \mathcal{P}$  consists of  $7 \times 7$  equidistant distributed parameters and  $\mathcal{S}_{\Omega} \subset \Omega$  is a randomly chosen set of  $2^{14}$  points. In order to apply Corollary 4.8, we define  $\square := (0, 4) \times (0, 1)$  and  $\circ := (0, 4) \times (0, 1/2) = \Omega_2$  as well as

$$\begin{aligned} \langle r_{\square}(\Phi^{\theta}(\mu)), v \rangle_{H_0^1(\square)} &:= \langle r_{\Omega}(\Phi^{\theta}(\mu)), v \rangle_{H_0^1(\square)}, & \forall v \in H_0^1(\square), \\ \langle r_{\circ}(\Phi^{\theta}(\mu)), v \rangle_{H_0^1(\circ)} &:= \langle r_{\Omega}(\Phi^{\theta}(\mu)), E_{\Omega} v \rangle_{H_0^1(\Omega)}, & \forall v \in H_0^1(\circ). \end{aligned}$$

It is readily seen that  $r_{\Omega}(\Phi^{\theta}(\mu))$  is well-defined on  $H_0^1(\square)$  and is an element of the dual space, which means in this example  $\mathcal{Z}'(\square) := (H_0^1(\square))'$ . Furthermore,  $r_{\square}(\Phi^{\theta}(\mu))$  is an extension of  $R'_{\Omega \rightarrow \square} r_{\Omega}(\Phi^{\theta}(\mu))$ , because  $r_{\square}(\Phi^{\theta}(\mu)) \equiv R'_{\Omega \rightarrow \square} r_{\Omega}(\Phi^{\theta}(\mu))$  on  $\mathcal{U}(\square)$ , defined in (4.5). With the space  $\mathcal{V}(\Omega)$  defined in (4.7) we define  $r_{\circ}(\Phi^{\theta}(\mu)) := E'_{\circ \leftarrow \Omega}(r_{\Omega}(\Phi^{\theta}(\mu)|_{\mathcal{V}(\Omega)}))$ . Then, Corollary 4.8 applies and with the constants from Example 3.1 we get

$$\frac{\|r_{\circ}(\Phi^{\theta}(\mu))\|_{H^{-1}(\circ)}}{2 \max\{\mu_1, \mu_2\}} \leq \|\nabla u(\mu) - \nabla \Phi^{\theta}(\mu)\|_{L_2(\Omega)} \leq \frac{\|r_{\square}(\Phi^{\theta}(\mu))\|_{H^{-1}(\square)}}{\min\{\mu_1, \mu_2\}}.$$

We use these constants in our experiments.

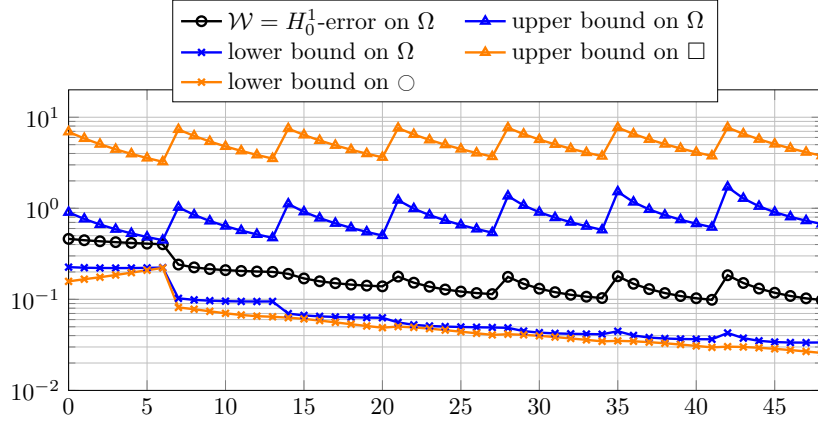


FIGURE 2. Absolute  $H_0^1$ -error as well as the estimated  $H_0^1$ -error on  $\Omega$ ,  $\square$  and  $\circ$ . The horizontal axis corresponds to the number  $N(i, j) \in \mathbb{N}$  of data points  $(\mu_i, \mu_j) \in \mathcal{S}_{\mathcal{P}}$ .

We show the results of this experiment in Figure 2. Although the parameter space is two-dimensional, we enumerated the parameters  $(\mu_i, \mu_j) \in \mathcal{S}_{\mathcal{P}}$  and plot the values against the number  $N(i, j) \in \mathbb{N}$  of the parameters. The comparison of the exact error (in black) with the upper and lower Riesz bounds on  $\Omega$  (blue) show that these bounds differ by a multiplicative factor up to 10. Recall that this is the best we can achieve with our error estimators (in orange). The lower bound is remarkably sharp. Recall that  $\circ = \Omega_2$ , which excludes all saw-blades. Due to the fact that the data functions are arbitrarily smooth on  $\circ$ , the computation of the lower bound with the spectral method converges exponentially fast and is thus very efficient.

The upper bound follows the line of the Riesz-bound on  $\Omega$  and is too pessimistic by another multiplicative factor of 10. A better fine-tuning of the involved constants might improve this upper bound.

**5.2. A parametric domain.** Our next numerical experiment is particularly suited for domain embedding, namely a linear elliptic PDE, posed on a domain  $\Omega_\mu$  with parameterized boundary shown in Figure 3. It is the unit square with a cutout, which cannot be smoothly transformed into a reference domain, due to the sharp corners for angles  $\mu > 0$ . Such a situation occurs e.g. in geometry optimization, where PINNs have already been used, [38].

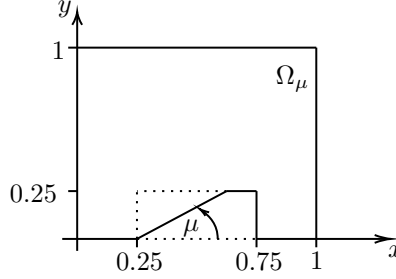


FIGURE 3. A parameterized square, where the parameter  $\mu$  is the angle of a recess.

When solving a PDE on  $\Omega_\mu$  with the finite element method, re-meshing might be necessary for different  $\mu$ . On the other hand, the training of a PINN is straightforward by excluding all points outside of the domain. This shows why a PINN might be an attractive tool for a PDE on  $\Omega_\mu$ .

Since the underlying domain is parameterized, we can consider a non-parametric elliptic equation of the form

$$\langle r_{\Omega_\mu}(u_\mu), v \rangle_{H_0^1(\Omega_\mu)} := (A \nabla u_\mu, \nabla v)_{L_2(\Omega_\mu)} + (b \cdot \nabla u_\mu + c u_\mu, v)_{L_2(\Omega_\mu)} - f_\mu(v) = 0,$$

for all  $v \in H_0^1(\Omega_\mu)$  with the diffusion, convection and reaction coefficients given by

$$A \equiv \begin{pmatrix} 1/2 & 1/4 \\ 1/4 & 1/2 \end{pmatrix}, \quad b \equiv \begin{pmatrix} 10 \\ -3 \end{pmatrix} \quad \text{and} \quad c(x, y) := xy + 1.$$

The source function is defined by  $f_\mu(v) := (10, v)_{L_2(\Omega_\mu)}$ . We choose the training set  $\mathcal{S}_{\Omega_\mu}$  as  $2^{16}$  random points in  $\Omega_\mu$ . The parameter training set  $\mathcal{S}_\mathcal{P}$  consists of five equidistant points in  $\mathcal{P} = [0, \pi/2]$ ,  $P = 1$ . The extended domain is chosen as  $\square := (0, 1)^2$  and the imbedded domain as  $\circ := (0, 1) \times (0.25, 1)$ .

The extension and restriction of the residual  $r_{\Omega_\mu}(u_\mu)$  can be done as in the previous example, Corollary 4.8 applies and yields the error estimate

$$\frac{\|r_\circ(\Phi^\theta(\mu))\|_{H^{-1}(\circ)}}{\|A\|_{L_\infty} + \|b\|_{L_\infty} + \|c\|_{L_\infty}} \leq \|\nabla u_\mu - \nabla \Phi^\theta(\mu)\|_{L_2(\Omega)} \leq \frac{\|r_\square(\Phi^\theta(\mu))\|_{H^{-1}(\square)}}{\lambda_{\min}(A)},$$

from which we deduce the constants.

The results for a set of nine parameters, which serve as the test set for the PINN, are depicted in Figure 4. The Riesz bounds on  $\Omega_\mu$  (blue) follow the slope of the exact error (black), the upper bound being quite sharp, the lower one too optimistic by a factor of about 10. The lower bound for the error estimator (orange), calculated on  $\circ$ , follows the slope and is quite sharp. The reason might be that the cut-off region does neither concern the Riesz lower bound nor the one on  $\circ$ . On the other hand, however, the upper bound does not follow the slope of the error and is too pessimistic by a factor of 10 – which overall seems acceptable, but is by far worse

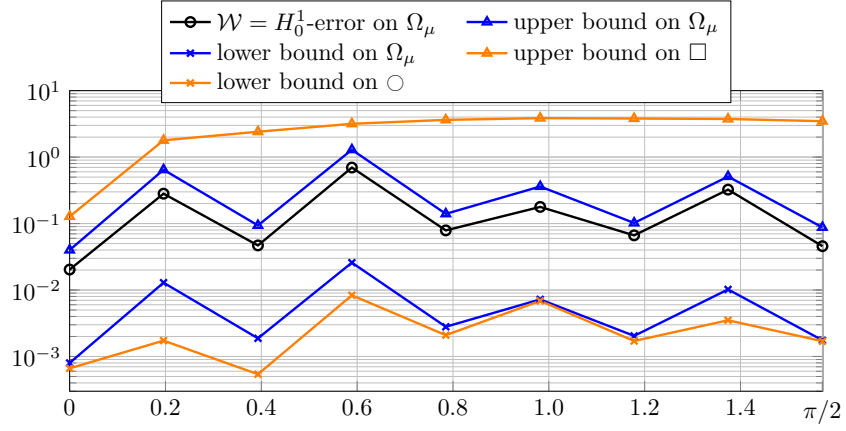


FIGURE 4. Absolute  $H_0^1$ -error as well as the estimated  $H_0^1$ -error on  $\Omega$ ,  $\square$  and  $\circ$ . The horizontal axis corresponds to the angle  $\mu$ .

than the Riesz upper bound on  $\Omega_\mu$ . The change of the geometry obviously has only a small effect on the proposed upper error bound.

**5.3. A parabolic problem on a non-convex polytope.** Finally, we report results for a time-dependent problem on a domain with “complicated” geometry. To this end, consider the parameterized parabolic problem  $\dot{u}_\mu + A_\mu u_\mu = f$ ,  $u_\mu(0) = 0$  on  $Q := I \times \Omega$ ,  $I := (0, 1)$  being the time horizon and  $\Omega \subset \mathbb{R}^2$  is the map of the state of Arkansas (USA) depicted in Figure 5. The domain is a non-convex polytope and therefore has a Lipschitz-boundary. Moreover,  $\Omega$  has sharp corners on the right- and lower left-hand side. The parametric elliptic operators  $A_\mu \in \mathcal{L}(H_0^1(\Omega), H^{-1}(\Omega))$  are

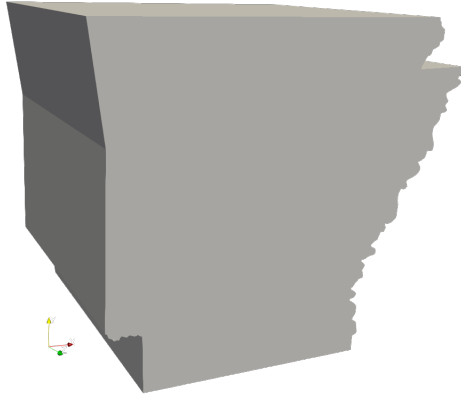


FIGURE 5. The space-time domain  $Q = I \times \Omega$ , where the green axis refers to the time.

defined by the variational form

$$\langle A_\mu \varphi, \psi \rangle_{H_0^1(\Omega)} := (K \nabla \varphi, \nabla \psi)_{L_2(\Omega)} + (b_\mu \nabla \varphi + c \varphi, \psi)_{L_2(\Omega)}, \quad \forall \varphi, \psi \in H_0^1(\Omega),$$



where the time-independent coefficient functions are chosen as

$$K \equiv \begin{pmatrix} 1 & 0 \\ 0 & 0.1 \end{pmatrix}, \quad b_\mu(x, y) := (31 - \mu) \begin{pmatrix} \sin^2(2y) \\ \cos((x+1)^{\mu/4}) \end{pmatrix} \quad \text{and} \quad c(x, y) := xy + 1,$$

with the parameter set  $\mathcal{P} := [1, 10] \subset \mathbb{R}$ ,  $P = 1$ . The parameter dependent convection is chosen to be *not* affinely decomposable, so that this standard assumption of the reduced basis method is not valid, see e.g. [39], and using a PINN seems attractive. We use the space-time variational formulation of the parabolic PDE as introduced in Example 3.2 above.

The height of Arkansas is normalized to 1 and the front upper left corner is located at  $(0, 1, 0)^T \in \mathbb{R}^3$ , so that we define  $\square := (0, 1.2) \times (0, 1)$  and  $\circ := (0.1345, 0.783) \times (0, 1) \subset \Omega$ . With this setting, the extension operator from Proposition 4.9 can be used and Corollary 4.10 applies.

The PINN has again been trained with a high-fidelity finite-element solution using training sets  $\mathcal{S}_Q$ , consisting of  $1.5 \cdot 10^5$  points for the space-time domain  $Q$  and  $\mathcal{S}_\mathcal{P}$ , consisting of 16 equidistant points for the parameter. The error has been measured on 31 parameters.

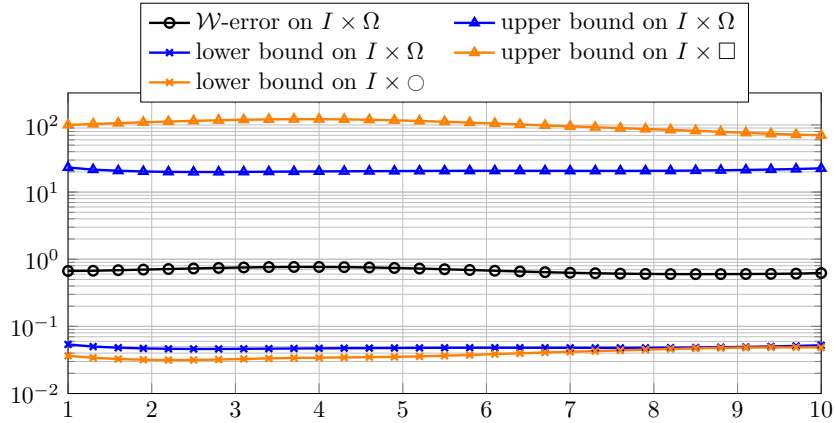


FIGURE 6. Absolute  $\mathcal{W}$ -error as well as the estimated  $\mathcal{W}$ -error on  $I \times \Omega$ ,  $I \times \square$  and  $I \times \circ$ . The horizontal axis corresponds to the parameter value  $\mu \in \mathcal{P}$ .

The results are depicted in Figure 6. The error of the PINN approximation does not depend much on the parameter  $\mu$ . This is also reflected by the bounds, so that they are basically multiples of the true error. The Riesz bounds on  $Q = I \times \Omega$  are about a factor 10 off the true error (black). This is due to the constants in the error-residual relation, see [27, Thm. 5.1] and the appendix therein. The error bounds (orange) are quite sharp, in particular the lower one. Again, the data is smooth on  $I \times \circ$ , so that we can use an efficient spectral method as we do not need to resolve the complicated geometry of  $\Omega$ .

**5.4. Computational times.** In order to investigate the computational overhead required for the lower and upper bounds, we collect in Table 1 the CPU/GPU times for (i) the PINN training, (ii) the evaluation of the PINN at the points  $\{\mu\} \times \mathcal{S}_\Omega$  for one  $\mu \in \mathcal{S}_\mathcal{P}$  and (iii) solving the Riesz representation problems on  $\circ$  and  $\square$

Problem	Training	Evaluation	Error estimation	
			$\circ$	$\square$
saw-blade	1241.52	0.0019	0.011	0.16
parametric domain	926.76	0.0128	0.011	0.15
Arkansas	7536.71	0.0720	2.249	1.77

TABLE 1. Times (in seconds) for training (GPU), PINN evaluation (GPU) and error estimation (CPU) on  $\circ$  and  $\square$ .

also for one  $\mu \in \mathcal{S}_{\mathcal{P}}$ . The times with respect to all  $\mu \in \mathcal{S}_{\mathcal{P}}$  scale linearly. The time measurement has been carried out using standard devices for each task, e.g., a NVIDIA Tesla V100 GPU has been used for the training and the evaluation of the PINN. The termination criterion of the training process has been a maximum number of iterations, which was  $5 \cdot 10^3$  in the case of the saw-blade domain and  $10^4$  iterations for the parametric and Arkansas domain. The evaluation of the error estimator on  $\square$  has been parallelized using two Intel Xeon Gold 6230 CPUs with 20 cores each. For the discretization, we have used standard  $P1$ -finite elements with around  $2.5 \cdot 10^5$  degrees of freedom. The Riesz problems on  $\circ$  have been solved with the spectral method using a nodal Lagrange basis of order 12 in the 2D cases and of order 8 in the time-dependent case. This leads to small dense linear systems, which can be solved using serial direct solvers and the error can be expected to be near machine accuracy, due to the exponential convergence of spectral methods. In case of the Arkansas domain the matrix size was  $729 \times 729$  and  $169 \times 169$  in the stationary cases. Thus, the comparable long solving time of 2.249 seconds may be due to the non-optimal internal routines of FEniCSx.

We can see that the time for the error estimation is negligible in comparison to the training time. Moreover, the lower bound on  $\circ$  can be computed efficiently and this can even be improved if one would use specialized spectral solvers. The numbers confirm the efficiency of the method, even though we did not even use a highly optimized implementation, but the standard algorithms within the FEniCSx implementation.

## 6. SUMMARY AND OUTLOOK

In this work, we introduced a novel framework for rigorously certifying the accuracy of Physics-Informed Neural Networks (PINNs) through a posteriori error estimation. Our method constructs efficiently computable error bounds independent of the PINN training process or the choice of loss function.

The idea is to extend and restrict the residual to a simpler domain, we derived both upper and lower error bounds that have been shown to be relatively sharp while enhancing computational efficiency. This is achieved by replacing the potentially complex problem domain by a simpler reference domain and by establishing relationships between functionals defined w.r.t. the corresponding spaces on the embedded domains. These relationships yield the desirable bounds, accessed by evaluation of dual norm estimates using Riesz representation as an alternative to using wavelet methods as introduced in [9].

Our numerical experiments validate the proposed certification framework for parameter-dependent linear elliptic and time-dependent parabolic PDEs. For a parameter-dependent diffusion problem on a non-convex domain, the evaluation of error bounds is greatly simplified by posing the computations on a much simpler domain with a limited but forgiving loss of sharpness. In the case of an elliptic

PDE with a parameterized boundary, our framework efficiently certifies PINN approximations without requiring a re-meshing for each parameter. Similarly, for a linear parabolic equation in a simultaneous space-time variational formulation, our method successfully extends to Bochner spaces.

Our numerical experiments provide one possible extension of residual functionals, and further refinements can be made by leveraging Hahn-Banach-type extensions, particularly in Hilbert spaces, leading to potentially sharper estimates. Moreover, the extension operator used here is optimal for  $\mathcal{V} = L_2$ , motivating the use of a first-order system formulation. This ensures that the residual remains in  $L_2(\Omega)$ , improving the accuracy of the certification. Ongoing work includes adaptive wavelet-based approximations in  $W_0^{m,p}(\square)$ , allowing for error certification in Banach spaces beyond Hilbert settings. A key direction for our future research is to extend the methodology to nonlinear PDEs, where error certification is more challenging but crucial for practical applications.

*Acknowledgement.* The authors acknowledge support by the state of Baden-Württemberg through bwHPC, and the Hellenic Foundation for Research and Innovation (H.F.R.I.) under the “2nd Call for H.F.R.I. Research Projects to support Post-Doctoral Researchers” (project number: 01247).

## REFERENCES

- [1] M. Dissanayake and N. Phan-Thien, “Neural-network-based approximations for solving partial differential equations,” *Comm. Numer. Methods Engrg.*, vol. 10, pp. 195–201, 1994.
- [2] I. Lagaris, A. Likas, and D. Papageorgiou, “Neural-network methods for boundary value problems with irregular boundaries,” *IEEE Trans. Neural Netw.*, vol. 11, pp. 1041–1049, 2000.
- [3] I. Lagaris, A. Likas, and D. Fotiadis, “Artificial neural networks for solving ordinary and partial differential equations,” *IEEE Trans. Neural Netw.*, vol. 9, pp. 987–1000, 2000.
- [4] M. Raissi and G. E. Karniadakis, “Hidden physics models: Machine learning of nonlinear partial differential equations,” *J. Comput. Phys.*, vol. 357, pp. 125–141, 2018.
- [5] M. Raissi, P. Perdikaris, and G. Karniadakis, “Physics-informed neural networks: A deep learning framework for solving forward and inverse problems involving nonlinear partial differential equations,” *J. Comput. Phys.*, vol. 378, pp. 686–707, 2019.
- [6] S. Mishra and R. Molinaro, “Estimates on the generalization error of physics-informed neural networks for approximating PDEs,” *IMA J. Numer. Anal.*, vol. 43, pp. 1–43, 01 2022.
- [7] T. De Ryck, A. D. Jagtap, and S. Mishra, “Error estimates for physics-informed neural networks approximating the navier–stokes equations,” *IMA J. Numer. Anal.*, vol. 44, pp. 83–119, 01 2023.
- [8] S. Berrone, C. Canuto, and M. Pintore, “Solving PDEs by variational physics-informed neural networks: an a posteriori error analysis,” *Annali Univ. Ferrara*, vol. 68, no. 2, pp. 575–595, 2022.
- [9] L. Ernst and K. Urban, “A certified wavelet-based physics-informed neural network for the solution of parameterized partial differential equations,” *IMA J. Numer. Anal.*, vol. 45, no. 1, pp. 494–515, 2025.
- [10] J. A. A. Opschoor, P. C. Petersen, and C. Schwab, “First order system least squares neural networks,” *arXiv math.NA*, no. eprint 2409.20264, 2024.
- [11] H. Monsuur, R. Smeets, and R. Stevenson, “Quasi-optimal least squares: Inhomogeneous boundary conditions, and application with machine learning,” *arXiv math.NA*, no. eprint 2412.05965, 2024.
- [12] B. Hillebrecht and B. Unger, “Certified machine learning: A posteriori error estimation for physics-informed neural networks,” in *2022 International Joint Conference on Neural Networks (IJCNN)*, pp. 1–8, 2022.

- [13] M. Bachmayr, W. Dahmen, and M. Oster, “Variationally Correct Neural Residual Regression for Parametric PDEs: On the Viability of Controlled Accuracy,” *arXiv, eprint 2405.20065*, 2024.
- [14] J. Berner, P. Grohs, G. Kutyniok, and P. Petersen, *The Modern Mathematics of Deep Learning*, pp. 1–111. Cambridge University Press, 2022.
- [15] R. Gribonval, G. Kutyniok, M. Nielsen, and F. Voigtlaender, “Approximation Spaces of Deep Neural Networks,” *Constr. Approx.*, vol. 55, no. 1, pp. 259–367, 2022.
- [16] P. Petersen and F. Voigtlaender, “Optimal approximation of piecewise smooth functions using deep ReLU networks,” *Neural Networks*, vol. 108, pp. 296–330, 2018.
- [17] K. Hornik, “Approximation capabilities of multilayer feedforward networks,” *Neural Networks*, vol. 4, no. 2, pp. 251–257, 1991.
- [18] K. Hornik, M. Stinchcombe, and H. White, “Multilayer feedforward networks are universal approximators,” *Neural Networks*, vol. 2, pp. 359–366, Jan. 1989.
- [19] I. Gühring, G. Kutyniok, and P. Petersen, “Error bounds for approximations with deep ReLU neural networks in  $W^{s,p}$  norms,” *Analysis and Applications*, vol. 18, pp. 803–859, Sept. 2019.
- [20] N. Sukumar and A. Srivastava, “Exact imposition of boundary conditions with distance functions in physics-informed deep neural networks,” *CMAME*, vol. 389, p. 114333, 2022.
- [21] J. Berg and K. Nyström, “A unified deep artificial neural network approach to partial differential equations in complex geometries,” *Neurocomputing*, vol. 317, pp. 28–41, Nov. 2018.
- [22] Z. Mao, A. D. Jagtap, and G. E. Karniadakis, “Physics-informed neural networks for high-speed flows,” *CMAME*, vol. 360, p. 112789, Mar. 2020.
- [23] S. Cai, Z. Wang, S. Wang, P. Perdikaris, and G. E. Karniadakis, “Physics-informed neural networks for heat transfer problems,” *Journal of Heat Transfer*, vol. 143, Apr. 2021.
- [24] S. Cai, Z. Mao, Z. Wang, M. Yin, and G. E. Karniadakis, “Physics-informed neural networks (pinns) for fluid mechanics: a review,” *Acta Mech. Sin.*, vol. 37, no. 12, pp. 1727–1738, 2021.
- [25] H. Hu, L. Qi, and X. Chao, “Physics-informed neural networks (pinns) for computational solid mechanics: Numerical frameworks and applications,” *Thin-Walled Structures*, vol. 205, p. 112495, 2024.
- [26] R. Lions, *Mathematical analysis and numerical methods for science and technology: Evolution problems I*, vol. 5. Springer, 2000.
- [27] C. Schwab and R. Stevenson, “Space-time adaptive wavelet methods for parabolic evolution problems,” *Math. Comp.*, vol. 78, no. 267, pp. 1293–1318, 2009.
- [28] N. Chegini and R. P. Stevenson, “Adaptive wavelet schemes for parabolic problems: Sparse matrices and numerical results,” *SIAM J. Numer. Anal.*, vol. 49, no. 1, pp. 182–212, 2011.
- [29] K. Urban and A. T. Patera, “An improved error bound for reduced basis approximation of linear parabolic problems,” *Math. Comp.*, vol. 83, no. 288, pp. 1599–1615, 2014.
- [30] J.-P. Aubin, *Applied functional analysis*. John Wiley & Sons, 2011.
- [31] V. Kadets, *A course in functional analysis and measure theory*. Springer, 2018.
- [32] R. A. Adams and J. J. Fournier, *Sobolev spaces*. Elsevier, 2003.
- [33] Y. Abramovich and C. Aliprantis, *An Invitation to Operator Theory*. American Mathematical Society, Sept. 2002.
- [34] C. Canuto, M. Y. Hussaini, A. Quarteroni, and T. A. Zang, *Spectral Methods: Fundamentals in Single Domains*. Springer Berlin Heidelberg, 2006.
- [35] I. A. Baratta, J. P. Dean, J. S. Dokken, M. Habera, J. S. Hale, C. N. Richardson, M. E. Rognes, M. W. Scroggs, N. Sime, and G. N. Wells, “DOLFINx: The next generation FEniCS problem solving environment,” 2023.
- [36] A. Paszke, S. Gross, F. Massa, A. Lerer, J. Bradbury, G. Chanan, T. Killeen, Z. Lin, N. Gimelshein, L. Antiga, A. Desmaison, A. Kopf, E. Yang, Z. DeVito, M. Raison, A. Tejani, S. Chilamkurthy, B. Steiner, L. Fang, J. Bai, and S. Chintala, “Pytorch: An imperative style, high-performance deep learning library,” in *Advances in Neural Information Processing Systems 32* (H. Wallach, H. Larochelle, A. Beygelzimer, F. d’Alché-Buc, E. Fox, and R. Garnett, eds.), pp. 8024–8035, Curran Associates, Inc., 2019.
- [37] L. Ernst, “Certification for PINNs.” [https://github.com/LeErnst/Certification\\_for\\_PINNs.git](https://github.com/LeErnst/Certification_for_PINNs.git), 2025.
- [38] Y. Sun, U. Sengupta, and M. Juniper, “Physics-informed deep learning for simultaneous surrogate modeling and pde-constrained optimization of an airfoil geometry,” *CMAME*, vol. 411, p. 116042, 2023.

- [39] J. S. Hesthaven, G. Rozza, and B. Stamm, *Certified Reduced Basis Methods for Parametrized Partial Differential Equations*. Springer, 2016.

INSTITUTE FOR NUMERICAL MATHEMATICS, ULM UNIVERSITY, HELMHOLTZSTR. 20, 89081 ULM, GERMANY

*Email address:* `lewin.ernst@uni-ulm.de`

INSTITUTE OF APPLIED AND COMPUTATIONAL MATHEMATICS, FOUNDATION OF RESEARCH AND TECHNOLOGY, NIKOLAOU PLASTIRA 100, VASSILIKA VOUTON, GR 70013 HERAKLION, CRETE, GREECE

*Email address:* `n.rekatsinas@iacm.forth.gr`

INSTITUTE FOR NUMERICAL MATHEMATICS, ULM UNIVERSITY, HELMHOLTZSTR. 20, 89081 ULM, GERMANY

*Email address:* `karsten.urban@uni-ulm.de`